PROCEEDINGS OF SCIENCE

The Silicon Vertex Detector of the Belle II experiment

A.B. Kaliyar ,[a,*] K. Adamczyk,[b] L. Aggarwal,[c] H. Aihara,[d] T. Aziz,[e] S. Bacher,[b] S. Bahinipati,[f] G. Batignani,[g,h] J. Baudot,[i] P. K. Behera,[j] S. Bettarini,[g,h] T. Bilka,[k] A. Bozek,[b] F. Buchsteiner,[a] G. Casarosa,[g,h] L. Corona,[h] S. B. Das,[l] G. Dujany,[i] C. Finck,[i] F. Forti,[g,h] M. Friedl,[a] A. Gabrielli,[m,n] B. Gobbo,[n] S. Halder,[e] K. Hara,[o,p] S. Hazra,[e] T. Higuchi,[q] C. Irmler,[a] A. Ishikawa,[o,p] Y. Jin,[n] M. Kaleta,[b] J. Kandra,[k] K. H. Kang,[q] P. Kodyš,[k] T. Kohriki,[o] R. Kumar,[r] K. Lalwani,[l] K. Lautenbach,[t] R. Leboucher,[t] S. C. Lee,[s] J. Libby,[j] L. Martel,[i] L. Massaccesi,[g,h] G. B. Mohanty,[e] S. Mondal,[g,h] K. R. Nakamura,[o,p] Z. Natkaniec,[b] Y. Onuki,[d] F. Otani,[q] A. Paladino[A,g,h] E. Paoloni,[g,h] H. Park,[s] L. Polat,[t] K. K. Rao,[e] I. Ripp-Baudot,[i] G. Rizzo,[g,h] Y. Sato,[o] C. Schwanda,[a] J. Serrano,[t] T. Shimasaki,[q] J. Suzuki,[o] S. Tanaka,[o,p] H. Tanigawa,[d] F. Tenchini,[g,h] R. Thalmeier,[a] R. Tiwary,[e] T. Tsuboyama,[o] Y. Uematsu,[d] L. Vitale,[m,n] Z. Wang,[d] J. Webb,[u] O. Werbycka,[n] J. Wiechczynski,[b] H. Yin[a] and L. Zani[B,t]

[a] *Institute of High Energy Physics, Austrian Academy of Sciences, 1050 Vienna, Austria*
[b] *H. Niewodniczanski Institute of Nuclear Physics, Krakow 31-342, Poland*
[c] *Panjab University, Chandigarh 160014, India*
[d] *Department of Physics, University of Tokyo, Tokyo 113-0033, Japan*
[e] *Tata Institute of Fundamental Research, Mumbai 400005, India*
[f] *Indian Institute of Technology Bhubaneswar, Bhubaneswar 752050, India*
[g] *Dipartimento di Fisica, Università di Pisa, I-56127 Pisa, Italy,* [A]*presently at INFN Sezione di Bologna, I-40127 Bologna, Italy*
[h] *INFN Sezione di Pisa, I-56127 Pisa, Italy*
[i] *IPHC, UMR 7178, Université de Strasbourg, CNRS, 67037 Strasbourg, France*
[j] *Indian Institute of Technology Madras, Chennai 600036, India*
[k] *Faculty of Mathematics and Physics, Charles University, 121 16 Prague, Czech Republic*
[l] *Malaviya National Institute of Technology Jaipur, Jaipur 302017, India*
[m] *Dipartimento di Fisica, Università di Trieste, I-34127 Trieste, Italy*
[n] *INFN Sezione di Trieste, I-34127 Trieste, Italy*
[o] *High Energy Accelerator Research Organization (KEK), Tsukuba 305-0801, Japan*
[p] *The Graduate University for Advanced Studies (SOKENDAI), Hayama 240-0193, Japan*
[q] *Kavli Institute for the Physics and Mathematics of the Universe, University of Tokyo, Kashiwa 277-8583, Japan*
[r] *Punjab Agricultural University, Ludhiana 141004, India*
[s] *Department of Physics, Kyungpook National University, Daegu 41566, Korea*

[*]Speaker

[t] *Aix Marseille Université , CNRS/IN2P3, CPPM, 13288 Marseille, France,* [B] *presently at INFN Sezione di Roma Tre, I-00185 Roma, Italy*
[u] *School of Physics, University of Melbourne, Melbourne, Victoria 3010, Australia*
E-mail: abdulbasith.kaliyar@oeaw.ac.at

The Belle II silicon vertex detector (SVD) is a four-layer double-sided silicon strip detector installed within the Belle II detector located at KEK, Japan. The SVD has been operating smoothly and reliably since the start of data taking in March 2019. The data quality and radiation damage effects have been continuously monitored. In this article, we report the operational experience of SVD, reconstruction performance, and effects of beam background and radiation damage. We also discuss some of the recent efforts to improve the software robustness targeting the high luminosity scenario and hardware activities performed during the first long shutdown of the Belle II experiment.

6th International Conference on Technology and Instrumentation in Particle Physics (TIPP2023)
4 - 8 Sep 2023
Cape Town, Western Cape, South Africa

1. Introduction

The Belle II experiment [1] aims to make precise measurements of weak-interaction parameters, study exotic hadrons, and search for physics beyond the Standard Model. The experiment is currently underway at the SuperKEKB accelerator research center located in Tsukuba, Japan. SuperKEKB [2] is an asymmetric-energy e^+e^- (4 GeV on 7 GeV) collider that operates at centre-of-mass energies near the $\Upsilon(4S)$ resonance (10.58 GeV). The peak luminosity achieved so far is 4.7×10^{34} cm^{-2}s^{-1}, which is the current world record. The ultimate target is to reach a peak luminosity of 6×10^{35} cm^{-2}s^{-1}. The Belle II detector, located around the collider interaction point, has so far collected 430 fb^{-1} of data. The eventual goal is to record 50 ab^{-1} of data in the next decade.

The vertex detector (VXD) is the innermost component in the Belle II detector system located closest to the interaction point. Comprising six layers, it includes two inner layers of silicon pixel detectors (PXD) [3], based on depleted field effect transistor sensors, and four outer layers of silicon strip detectors, known as the silicon vertex detector (SVD) [4]. The SVD is crucial for extrapolating the measured tracks to the PXD that point at a region of interest, which helps to significantly reduce the amount of data recorded by the PXD. Besides that, the SVD performs standalone tracking of low-momentum particles, vertex detection of K_S^0 and Λ particles, as well as contributes to the charged-particle identification by providing energy-loss information.

In July 2022, Belle II temporally paused operation for the first long shutdown to allow the accelerator maintenance and improvements to the detector. The VXD was reinstalled during this time with a new complete PXD and the same SVD. In this article, we present a detailed description of the SVD, its performance until July 2022, effects of radiation damage, the software improvements aimed towards high-luminosity running, and finally a report on the the VXD re-installation and commissioning during the long shutdown.

2. The Belle II Silicon Vertex Detector

The Belle II SVD is composed of four layers of double-sided silicon strip detectors (DSSD), namely layers 3, 4, 5, and 6, placed at radii of 39, 80, 104, and 135 mm, respectively, from the beam pipe. The material budget is about 0.7% of radiation length X_0 per layer. In total, there are 172 DSSD sensors representing an area of 1.2 m^2 and 224,000 readout strips. There are three types of DSSDs: small rectangular sensors in layer 3, large rectangular sensors in the barrel region of layers 4, 5, and 6, and slanted trapezoidal sensors to extend spatial coverage toward the forward region of these three outermost layers. These sensors are made from an N-type bulk 6-inch wafer with a thickness of about 300 μm. To provide two-dimensional spatial information, P-side strips of the sensors are placed parallel to the beam axis, while N-side strips are placed perpendicular to it. The details of the DSSDs are summarized in Table 1. The readout strips are AC coupled and there is one intermediate floating strip between two readout implants. The full depletion voltage ranges from 20 to 60 V, and the operating voltage is 100 V. The radiation hardness of SVD sensors is about 6 Mrad.

The SVD uses the APV25 [5] frontend readout ASIC, which has 128 input channels. It collects signals from the strips and provides an analog readout. APV25 has a fast 50 ns shaping time

Table 1: Details of the three types of DSSDs used in the SVD.

	Small rectangular	Large rectangular	Trapezoidal
Sensor active area (mm^2)	122.90×38.55	122.90×57.52	$122.76 \times (38.42 - 57.59)$
Number of P-strips	768	768	768
P-strip readout pitch (μm)	50	75	$50 - 75$
Number of N-strips	768	512	512
N-strip readout pitch (μm)	160	240	240
Thickness (μm)	320	320	300
Manufacturer	Hamamatsu	Hamamatsu	Micron

and a radiation hardness of up to 100 Mrad. By default, the chip operates in multipeak mode at a clock frequency of 31.8 MHz, which is 1/8th of the SuperKEKB bunch-crossing frequency. Six consecutive samples are read out upon the arrival of a global hardware trigger to reconstruct the signal pulses. To save the data transmission bandwidth during high-luminosity runs, a mixed operation mode is developed, where three or six samples are acquired depending on the timing precision of the hardware trigger. This 3/6-mixed operation mode has been tested and is ready to be deployed in the future.

3. Operation and performance

The SVD has been operating smoothly and reliably since its installation in 2019. The total fraction of masked strips due to defects is less than 1% and only one out of 1748 APV25s was temporarily disabled. Temperature and calibration constants are evolving within the expected ranges due to radiation damage. The hit efficiency exceeds 99% for all the sensors. Figure 1 shows the distributions of signal cluster charge and cluster signal-to-noise ratio (SNR) of an example sensor measured in 2022 and 2020. The signal cluster charge is normalized to the track path length in the silicon to correct for the track's incidence angle. The normalized cluster charge is found to be in good agreement with expectations and similar across all sensors. The charge matches the expected minimum ionizing particle value of 24000 e^- within 15%, which is the uncertainty in the absolute APV25 gain calibration. We define the cluster SNR by dividing the total cluster charge by the quadratic sum of the noise values from each strip in the cluster. A small decrease in cluster SNR is observed in the 2022 data due to approximately 20−30% increased noise from radiation damage. All 172 DSSD sensors generally exhibit very good SNR, with most probable values typically falling within the range of 13 to 30, depending on sensor side and position.

The cluster-position resolution is crucial for vertexing and track reconstruction performance. The position resolution of the SVD is estimated from the residual between the cluster position and the unbiased track extrapolation, after subtracting quadratically the track extrapolation uncertainty [6]. Studies based on $e^+e^- \to \mu^+\mu^-$ events show a resolution of $7-12$ μm for the P-side and $15-25$ μm for the N-side. These are in fair agreement with expectations from the sensor pitch. Good stability of position resolution over time is also confirmed by comparing measurements from 2022 with those from 2020.

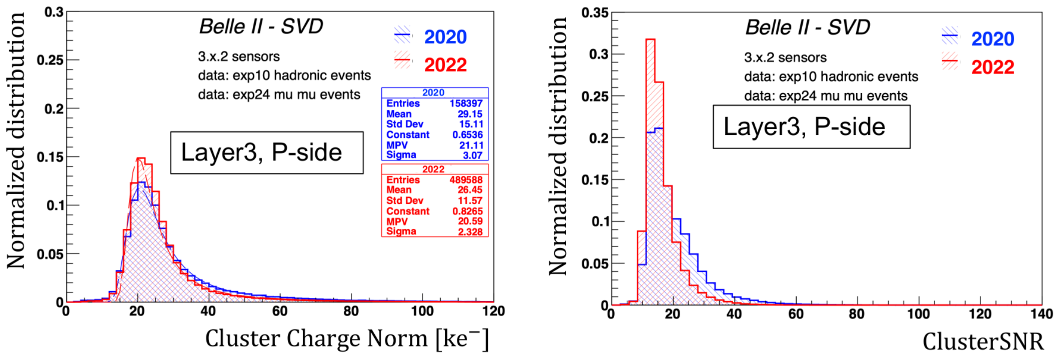

Figure 1: Distributions of signal cluster charge (left) and cluster SNR (right) for P-strips of a layer 3 sensor.

The SVD also offers excellent hit-time resolution. It is measured from the residuals between the hit time and the e^+e^- collision time provided by the central drift chamber of the Belle II detector. The measured hit-time resolution is 2.9 ns (2.4 ns) for the P (N) side. The hit-time information is also used to mitigate the machine-related background, which is typically unassociated with the e^+e^- collisions. This off-time-hit background enters the triggered-data acquisition window and increases the strip occupancy. Background occupancy above a certain threshold may cause tracking performance degradation. In the case of multiple particles crossing the sensor, we can use the time difference between the P- and N- side clusters to suppress the wrong combination of these clusters. By requiring the cluster time within the 50 ns of the event time and time difference between the P- and N-side clusters within 20 ns, 50% of the off-time background hits can be rejected while maintaining 99% tracking efficiency. This allows us to set the hit-occupancy limit of layer 3 to 4.7% without tracking performance deterioration.

We are currently developing two new algorithms that utilize the SVD time information to further relax the hit-occupancy limit and enhance offline software robustness in the high-background environment. One of these algorithms requires a selection of the tracktime, which is computed by combining the hit-time of SVD clusters associated with a track. This reduces the fake-track rate, thus relaxing the hit-occupancy limit. The second algorithm involves grouping SVD clusters based on the hit-time information. The cluster-time distribution has a clear grouping structure since clusters from different bunches are collected within the acquisition time window of the triggered event. While signal clusters are grouped around the event time, background hits, caused by neighboring beam-bunches, form other groups. It turns out that the hit-time selection cannot help to eliminate background hits present within the 50 ns window. The cluster grouping method allows event-by-event classification and further background suppression. The inclusion of these two algorithms allow us to set the hit-occupancy limit at around 6%. Further software improvement and optimization are currently ongoing before incorporating these features into the actual data processing.

4. Beam background and radiation effects

In this section, we discuss the impact of radiation damage on the SVD sensors during their operation. The beam-induced background increases the hit occupancy and causes radiation damage to the sensors. The radiation damage can affect the strip noise, leakage current, and full depletion voltage of sensors, so these quantities are constantly monitored during the operation. The current average hit occupancy on layer 3 sensors is less than 0.5% and well under control. We estimate the radiation dose in the SVD using the data from diamond sensors mounted on the beam pipe and the bellows pipes outside the VXD. The total integrated radiation dose on layer 3 sensors is 70 krad, which corresponds to an equivalent 1 − MeV neutron fluence of 1.6×10^{11} $\mathrm{n_{eq}/cm^2}$, assuming the ratio of a neutron fluence to a radiation dose of 2.3×10^{9} $\mathrm{n_{eq}/cm^2/krad}$ based on Monte-Carlo simulation.

During the operation, the strip noise, dominated by the interstrip capacitance, increases by about 20% (30%) for the N-side (P-side) and is expected to be saturated. The leakage current is gradually increasing; in general, its value shows a linear dependence on the accumulated dose, as expected from the non-ionising energy-loss model [7]. So far, this increase has had a negligible contribution to the noise because of the small leakage-current and short APV25 shaping time. However, after 6 Mrad, the leakage current contribution to the noise might become significant which can reduce the SNR below 10 in layer 3. So far no changes in full depletion voltage have been observed in the operating sensors.

We have carried out several irradiation campaigns to better evaluate the radiation tolerance of SVD sensors, even after bulk-type inversion. In July 2022, a new irradiation campaign of SVD sensors was performed with 90 MeV electron beam at the Research Center for Electron Photon Science of Tohoku University, with a radiation dose up to 10 Mrad (corresponding to a neutron fluence of 3×10^{13} $\mathrm{n_{eq}/cm^2}$). The type inversion of the sensor bulk is confirmed after 2 Mrad of radiation. The tests confirm that the SVD sensors work well even after the bulk-type inversion, as expected from previous experience with silicon detectors of similar type. These results provide a large safety margin for the SVD, even after a decade-long operation at the target luminosity.

5. VXD reinstallation during Long Shutdown 1

In July 2022, Belle II paused its operation for the first long shutdown to allow accelerator maintenance and implement upgrades to the detector. We installed a brand new pixel detector (PXD2) in the VXD volume, with a complete second layer, alongside the current SVD. The SVD crew engaged in intense hardware activities during the de-installation and re-installation of the VXD. On May 10, 2023, the VXD was safely extracted from the Belle II detector, followed by dismounting the two SVD half-shells from the old PXD and mounting them on the PXD2. All these delicate operations involved several steps with extensive testing of the detector and the environmental monitoring system, to ensure the healthiness of the system after each step. The healthiness of all SVD sensors was confirmed during the commissioning of the new VXD in the clean room. In July 2023, the new VXD was successfully reinstalled into the Belle II detector. Additional tests, including cosmic-ray runs, were performed before the start of the actual beam operation. After this shutdown, Belle II officially restarted data taking in January 2024, and so far, SVD is performing as smoothly as before.

6. Conclusion

The Belle II SVD has been taking high-quality data since March 2019. Operation is stable and reliable, with excellent detector performance. Effects from radiation damage are observed at the expected level; however, their contribution has not caused any degradation of the SVD tracking performance so far. During the first long shutdown, a new VXD was successfully re-installed into the Belle II detector, incorporating the new PXD2 together with the existing SVD.

We expect the SVD to remain safe even after a decade of operation, based on background extrapolation to the target high luminosity as well as the results of an irradiation campaign. However, the high-background environment in the future may deteriorate the SVD tracking performance, as indicated by simulation studies. Not only to improve the robustness against a high background, but also to adapt to a possible modification of the interaction region, technology assessment is ongoing for a possible VXD upgrade during the second long shutdown of Belle II [8–10].

7. Acknowledgements

This project has received funding from the European Union's Horizon 2020 research and innovation programme under the Marie Sklodowska-Curie grant agreements No 644294, 822070 and 101026516 and ERC grant agreement No 819127. This work is supported by MEXT, WPI and JSPS (Japan); ARC (Australia); BMBWF (Austria); MSMT (Czechia); CNRS/IN2P3 (France); AIDA-2020 (Germany); DAE and DST (India); INFN (Italy); NRF and RSRI (Korea); and MNiSW (Poland).

References

[1] T. Abe *et al.,* (Belle-II Collaboration), Belle II Technical Design Report [arXiv:1011.0352].

[2] Y. Ohnishi *et al.,* Prog. Theor. Exp. Phys. **2013**, 03A011 (2013).

[3] B. Wang *et al.,* (Belle-II DEPFET and PXD Collaborations), Nucl. Instrum. Meth. A **1032**, 166631 (2022).

[4] K. Adamczyk *et al.,* (Belle-II SVD Collaboration) JINST **17**, P11042 (2022).

[5] M. J. French *et al.,* Nucl. Instrum. Meth. A **466**, 359 (2001).

[6] R. Leboucher *et al.,* Nucl. Instrum. Meth. A **1033**, 166746 (2022).

[7] G. Lindström *et al.,* Nucl. Instrum. Meth. A **465**, 60 (2001).

[8] Belle-II Collaboration, Snowmass Whitepaper: The Belle II Detector Upgrade Program, [arXiv:2203.11349] (2022).

[9] M. Babeluk *et al.,* Nucl. Instrum. Meth. A **1048** 168015 (2023).

[10] A. Ishikawa *et al.,* Nucl. Instrum. Meth. A **978**, 164404 (2020).